441

Surface Reactions of Ethyl Groups on Clean and O-Modified Ru(001)

A. Kis, J. Kiss, D. Olasz, and F. Solymosi*

Reaction Kinetics Research Group of the Hungarian Academy of Sciences, University of Szeged, P.O. Box 168, H-6701 Szeged, Hungary

Received: November 30, 2001; In Final Form: March 7, 2002

The surface reactions of C_2H_5 species produced by thermal and UV photon-induced dissociation of C_2H_5I have been followed by means of temperature-programmed desorption and X-ray photoelectron spectroscopy. Cleavage of the C−I bond begins at 130 K on the clean surface. The primary products of thermal dissociation are adsorbed C_2H_5 and I. C_2H_5 groups take part in hydrogenation/dehydrogenation reactions forming C_2H_6 in gas-phase and adsorbed ethylidyne (CCH_3) on the surface. Preadsorbed O(a) exerts a significant stabilization influence on the dissociation and the desorption of the parent molecule. In its presence the amount of CCH_3 decreases and C_2H_4 appears in the desorbing products. In addition, oxygen atoms react with C_2H_5 to give diethyl ether and, at higher coverage, acetaldehyde. The decomposition of CCH_3(a) on the O-presaturated sample produces carbidic deposits (C, CH_x), which react with oxygen to form CO. UV illumination enhances the dissociation of the C−I bond and consequently the formation of CCH_3(a) on clean Ru(001), but the product distribution on an O-covered surface is not affected by irradiation.

1. Introduction

It has been recognized for a long time that the synthesis of hydrocarbons proceeds by the coupling and polymerization of the smallest hydrocarbon fragments on the catalyst surface. These hydrocarbon species (CH_2, CH_3, C_2H_5, etc.) play an important role in the partial and complete oxidation of hydrocarbons.[1] Halogenated hydrocarbons through their thermal and UV photon-induced dissociation were thought to be the most suitable sources for the preparation of this species.[2−6]

In our previous studies we examined the adsorption of CH_2I_2 on a Ru(001) surface with the aim of generating adsorbed CH_2 moieties.[7] CH_2 fragments, similar to CH_3 on this surface,[8] underwent self-hydrogenation into methane on one hand, and dimerization to CCH_3 via the formation of adsorbed ethylene on the other hand. Preadsorbed oxygen atoms reacted with CH_2 to give formaldehyde above 200 K.[9]

In the present work an account is given on the surface reaction of C_2H_5 generated by the dissociation of C_2H_5I on clean and oxygen-precovered Ru(001) surfaces. The surface chemistry of C_2H_5 produced by thermal dissociation of C_2H_5I had been studied previously on several metal surfaces. C_2H_5 groups take part in hydrogenation/dehydrogenation reactions on Pt(111),[10−12] Rh(111),[13] Pd(100),[14] and Mo_2C/Mo(111)[15] surfaces. C_2H_6 and C_2H_4 were detected among the desorption products. A certain fraction of adsorbed ethylene is transformed to adsorbed ethylidyne. The coupling of C_2H_5 into butane was not observed on the above-mentioned Pt metals. It was identified, however, on Ag(111),[16] Cu(111),[17] and Au(111)[18] surfaces. Oxidation of C_2H_5 was studied earlier on Rh(111).[19,20] The product distribution strongly depended on the oxygen coverage. Oxygen adatoms inhibited the dehydrogenation reaction and besides total oxidation it promoted the formation of aldehyde at high surface concentrations of oxygen.[19,20]

* Corresponding author. Fax: +36-62-424-997. E-mail: fsolym@chem.u-szeged.hu.

2. Experimental Section

2.1. Methods. The experiments were performed in an ultrahigh vacuum system with a background pressure of 5×10^{-10} mbar, produced by turbomolecular and ion-getter pumps. The chamber was equipped with an electrostatic hemispherical analyzer (Leybold-Hereaus LHS-10), an Al K_α X-ray anode for XPS, and an electron gun for AES measurements. All binding energies were referred to the Fermi level with the Ru($3d_{5/2}$) peak at 280.0 eV. XP spectra were smoothed by fast Fourier transform method. For TPD the sample was resistively heated at 5 K/s from 110 K to a selected temperature. The mass spectrometer was in "line of sight". Adsorbate-covered surfaces were irradiated, through a UV grade sapphire window, with a 40 W high-pressure Hg arc lamp (Photon Technology Inc.). The incident angle was 30° from the surface normal. The full spectrum of the Hg lamp gave 50 mW/cm^2 at the sample as measured with a power meter in a separate experiment outside the chamber. The maximum photon energy at the sample was not greater than 5.4 eV (the onset of UV intensity from the Hg arc lamp). At this maximum photon energy the photon flux was calculated to be 1×10^{16} cm^{-2} s^{-1}.

2.2. Materials. The surface of the Ru crystal (1.5 mm thick by 8.0 mm diameter) was oriented to within 0.5° of the (001) face and it was mechanically polished with diamond paste of different grain sizes. The crystal was spot welded to two 0.25 mm-diameter tantalum wires for resistive heating and was cooled to 110 K by heat conduction to a liquid nitrogen reservoir. To reach high temperature (1550 K) in the cleaning procedure, the sample was heated from the rear by the radiation of a tungsten filament. The temperature was measured with a chromel−alumel thermocouple spot welded to the side of the crystal.

Rigorous sample cleaning was done by Ar^+ bombardment to remove irreducible oxides and common impurities. Routine cleaning from surface carbon was accomplished by cycling the crystal temperature between 900 and 1450 K with an O_2 flux

10.1021/jp0142637 CCC: $22.00
Published on Web 05/01/2002

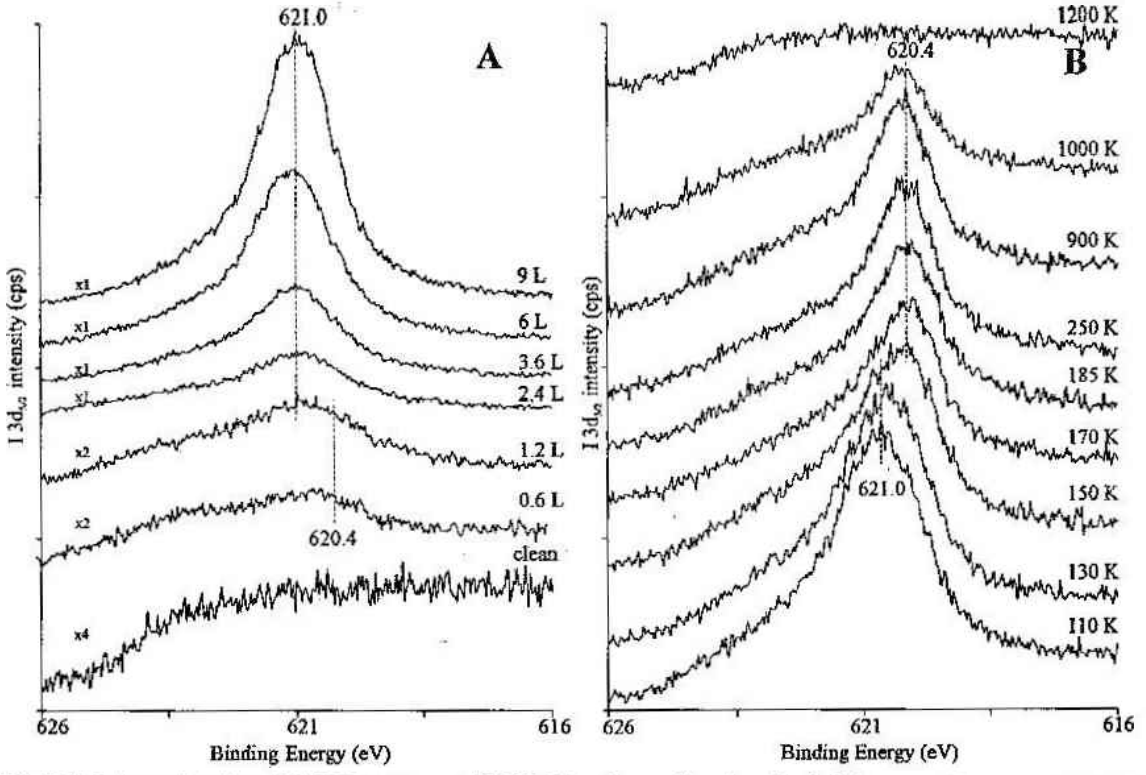

Figure 1. XPS of I($3d_{5/2}$) as a function of C_2H_5I exposure at 110 K (A) and annealing the adsorbed layer to different temperatures (B).

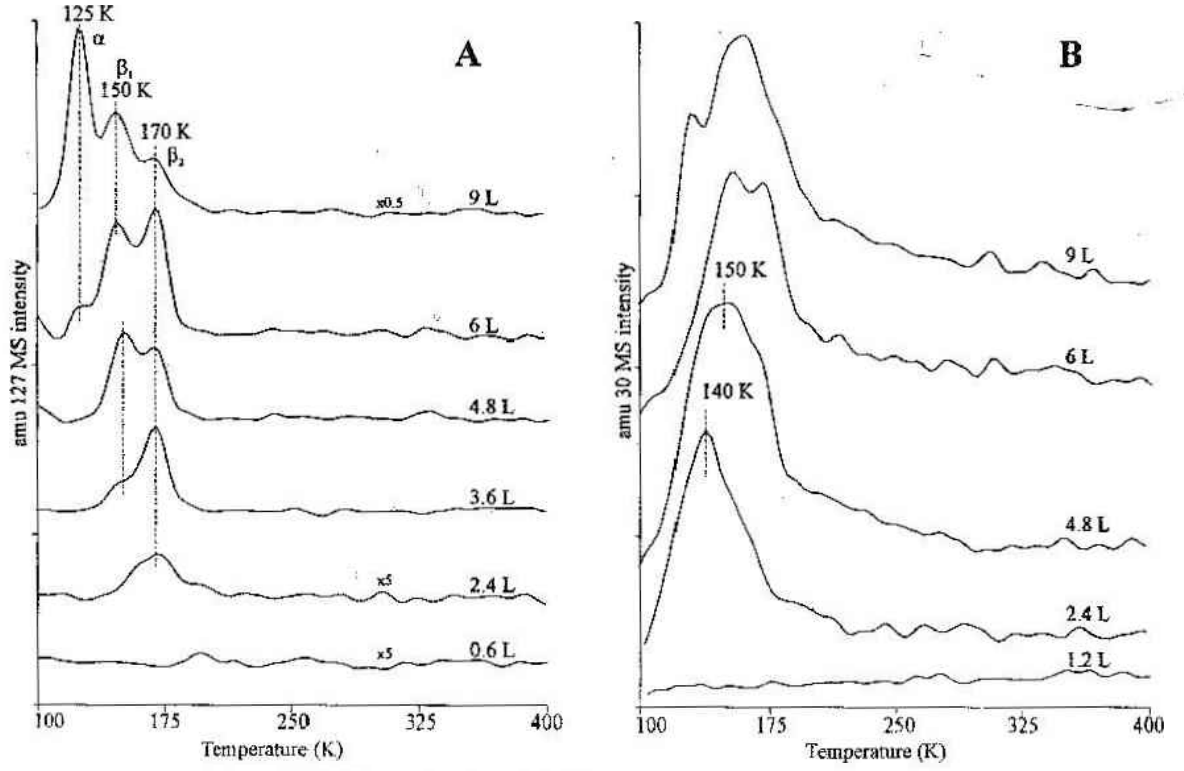

Figure 2. TPD spectra of C_2H_5I(A) and C_2H_6(B) as a function of C_2H_5I exposure. Adsorption temperature was 110 K.

which resulted in 1×10^{-8} Torr pressure rise as measured by the system's ion gauge. This was followed by annealing at 1550 K to remove adsorbed oxygen.

C_2H_5I was obtained from Fluka, it was degassed by freeze–pump–thaw cycles prior to use. Mass-spectrometric analysis did not show any contamination, only the fragments of C_2H_5I were detected. The O_2 was obtained from Messer-Griesheim. $^{18}O_2$ isotope was used in TPD measurements in order to assist the identification of different oxygenated products. The oxygen coverage was determined by the O(1s) XP signal which is calibrated against the ideal O coverage of p(1 × 2)-O (assumed to be 0.5 ML).[21]

3. Results

3.1. Clean Ru(001) Surface. Figure 1A shows the XP spectra of Ru(001) surface after the adsorption of different amounts of C_2H_5I at the adsorption temperature of 110 K. For the smallest exposures the I($3d_{5/2}$) signal appears at 620.4 eV, which shifts to 621.0 eV at and above 1.2 L exposure. This latter peak

TABLE 1: Summary of the Results of TPD Measurements after Adsorption of C_2H_5I at 110 K

products		T_P (K) clean	T_P (K) $\Theta_0 = 0.12-0.25$	T_P (K) $\Theta_0 = 0.5$	E_d[a] kJ/mol clean	E_d[a] kJ/mol $\Theta_0 = 0.25$	E_d[a] kJ/mol $\Theta_0 = 0.5$
C_2H_5I	α	125	125	125	29.9	29.9	29.9
	β_1	150			36.1		
	β_2	170	190	200	41.1	47.0	49.5
	γ		295	310		73.0	76.7
C_2H_6		140−150	285	315	37.1	70.5	77.9
C_2H_4			285	315		70.5	77.9
H_2 at 1 ML		290	285	330	71.9	70.5	81.6
		340			84.1		
		400			99.0		
CO			725	500		179.4	123.7
$(C_2H_5)O$			335			82.9	
CH_3CHO				405			100.2

[a] Assuming first-order process with 10^{13} s^{-1}.

dominates the iodine region of the XP spectra at monolayer coverage. Annealing the adsorbed layer resulted in a significant change in the XP spectra. The binding energy of the I($3d_{5/2}$) moves to lower value, 620.4 eV, from 130 K slightly above the adsorption temperature (Figure 1B). The fwhm is almost twice as large for the spectra taken between 130 and 170 K as that above this temperature. Above 170 K the peak retains its position up to 900 K where the desorption of atomic iodine begins.

The thermal desorption spectra of the C_2H_5I are shown in Figure 2A. Desorption of C_2H_5I is observed only from 2.4 L dose with a peak at T_P = 170 K (β_2). A small increase in the dose results in the appearance of new desorption peaks. The first one, labeled with β_1, appears at 3.6 L with a T_P = 150 K, the second one emerges from 6 L exposure at T_P = 125 K (α). The α peak does not saturate, while the β_1 and β_2 peaks attain their saturation values at 6 L dose. Their relative intensity is approximately 1.

Figure 2B shows the desorption of C_2H_6 following the 30 amu trace. The leading edge of the TPD curves begins slightly above the adsorption temperature. With increasing dose the peak temperature moves from 140 K to a bit higher value. This shift can be partly explained by the larger amount of the parent molecule among the desorption products as it possesses an 30 amu fragment. Iodine desorption was observed above 900 K, with a T_P = 1080 K at monolayer coverage (not shown). It is important to point out that no ethylene formation was detected by MS analysis.

TPD curves for H_2 desorption are plotted in Figure 3. The shape of the curve depends sensitively on the initial dose of C_2H_5I. A single asymmetric peak appears up to 2.4 L exposure with a tail extending to higher temperatures. The peak temperature shifts from 405 to 350 K with increasing exposure, meantime the integrated peak area doubles. A new feature develops on the low-temperature side of the TPD curve from 3.6 L exposure (T_P = 290 K). Neither the area nor the position of the peak changes. At the same time the intensity of the peak with T_P = 350 K reduces and at 6 L dose a shoulder emerges on its high-temperature side at 400 K. There is a broad desorption feature above 500 K which becomes more pronounced at higher exposures.

Characteristic TPD data are collected in Table 1.

3.2. Effects of UV Illumination. The primary aim of the UV irradiation study is to promote the generation of C_2H_5 at low temperature, where its decomposition and secondary reactions are minimal. The effect of illumination is exhibited by changes in the position of I($3d_{5/2}$) in XP spectra and post-irradiation TPD. Figure 4 shows the effect of illumination time on the position of the I($3d_{5/2}$) peak at around monolayer

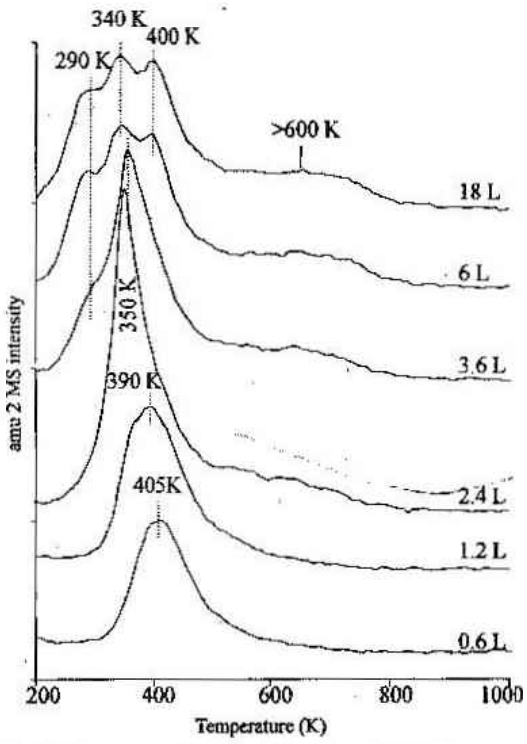

Figure 3. TPD spectra of H_2 as a function of C_2H_5I exposure.

coverage. The binding energy value clearly shifted from 621.0 eV to lower energy even after a relatively short irradiation. This shift was accompanied by a decrease of the peak area indicating that besides the C−I bond breaking some photoinduced desorption also occurred.

In harmony with this, the irradiation reduces the amount of C_2H_5I desorbed and caused the desorption peaks to shift to slightly higher temperatures. At the same time, the amount of C_2H_6 continuously decreased, and it was totally suppressed after 10 min irradiation (Figure 5A). The amount of the desorbed H_2 is also significantly reduced (by ~50%) and a new peak appeared at 470 K. Further illumination caused no change in the total integrated area of the desorption of H_2, but the peak at 470 K become more pronounced (Figure 5B). Attempt was made to detect other products (C_2H_4, C_4H_{10}), but none of them was found in the desorbing products.

3.3. Oxygen-Covered Ru(001). Figure 6A displays the effect of preadsorbed oxygen on the integrated area of the I($3d_{5/2}$) XP signal taken at 110 K. For comparison the values measured for clean surface are also plotted. The linearity of this curve shows that the sticking probability of C_2H_5I molecules does not change as a function of coverage. At low exposures the sticking coefficient is the same on both surfaces, but a small difference can be detected from 3.6 L dose.

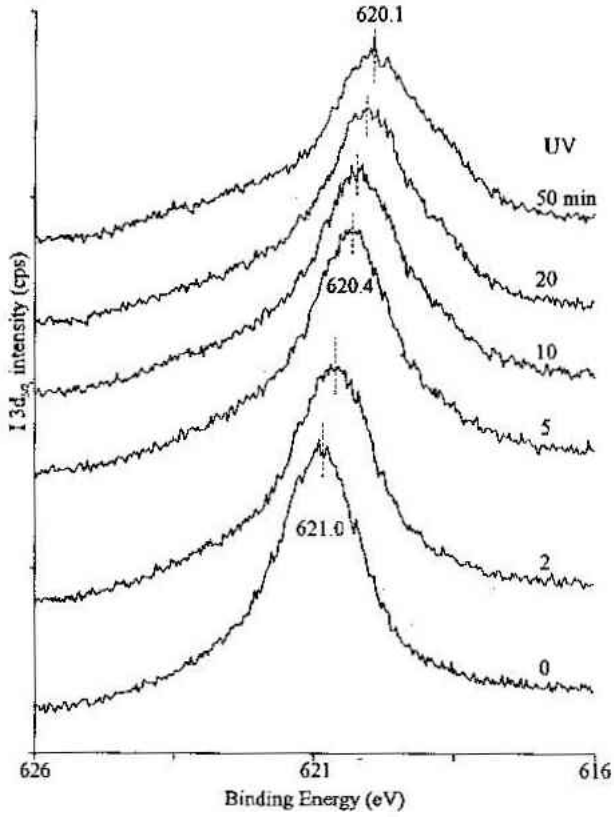

Figure 4. XP spectra of Ru(001) exposed to 6 L of C_2H_5I and irradiated with UV photons at 110 K.

The thermal stability of the C−I bond is significantly increased on the O-presaturated surface. The sharp shift of the I($3d_{5/2}$) XP signal of the O-modified sample begins above 250 K, i.e., 150 K higher than on the clean surface (Figure 6B). The different chemical environment accounts for the observed deviation of the I($3d_{5/2}$) binding energies (0.1 eV) for the clean and O-modified Ru(001) samples.

Figure 7A shows the desorption spectra of C_2H_5I as a function of O coverage. In agreement with the XPS results TPD measurements also indicate the presence of molecular C_2H_5I well above its desorption temperature from the clean surface. From $\Theta_O = 0.12$ ML a new desorption peak emerges above 200 K, its peak temperature shifts from 290 to 310 K with increasing the surface concentration of atomic oxygen.

The spectra following 30 amu traces are represented in Figure 7B. As the same desorption spectra were registered below 350 K at 29, 28, and 27 amu, we conclude that the desorption of C_2H_6 is responsible for the peaks observed. The feature at 140−150 K is suppressed above $\Theta_O = 0.06$ ML and new peak emerges at $T_P = 285-315$ K indicating the formation of C_2H_6 is shifted to higher temperature. There are, however, peaks at and above 500 K which were not observed at 29 and 28 amu. We attributed them to the desorption of $C^{18}O$.

In Figure 8A the amu 28 trace can be seen at different O coverages. Whereas on a clean surface the intensity ratio of amu 28 and 30 is 3.4, corresponding to the mass spectrum of C_2H_6, in the presence of coadsorbed O we obtained higher values, maximum 5.7. This clearly suggests the simultaneous formation of C_2H_4 and C_2H_6. Calculation showed that the ethylene/ethane ratio is approximately 1 at $\Theta_O = 0.12$, and it increased to 1.86 at $\Theta_O = 0.5$.

A significant alteration in the TPD spectra of H_2 occurred on the O-covered surface (Figure 8B). The $T_P = 350$ K peak with a shoulder splits into two separate peaks even at $\Theta_O = 0.06$ ML. Both peaks move to higher temperature ($T_P = 300$ and 460 K) with the rise of O coverage to 0.12 ML. The peak at 460 K disappears at $\Theta_O = 0.25$ ML, the spectra resembles the 30 and 28 amu traces between $\Theta_O = 0.25-0.5$ ML. The remaining peak at 300 K shifts to 330 K with increasing Θ_O. The change in the relative peak intensities as a function of Θ_O ($\Theta_O \geq 0.25$ ML) shows the same trend for 28, 30, and 2 amu traces.

Oxygenated hydrocarbons also appeared among the desorption products ($^{18}O_2$ was used in all experiments). Figure 9A represents the changes of the amu 31 trace. On the basis of the mass fragmentation pattern (amu 31 and 46), this species is attributed to acetaldehyde ($CH_3CH^{18}O$). The desorption of CH_3-

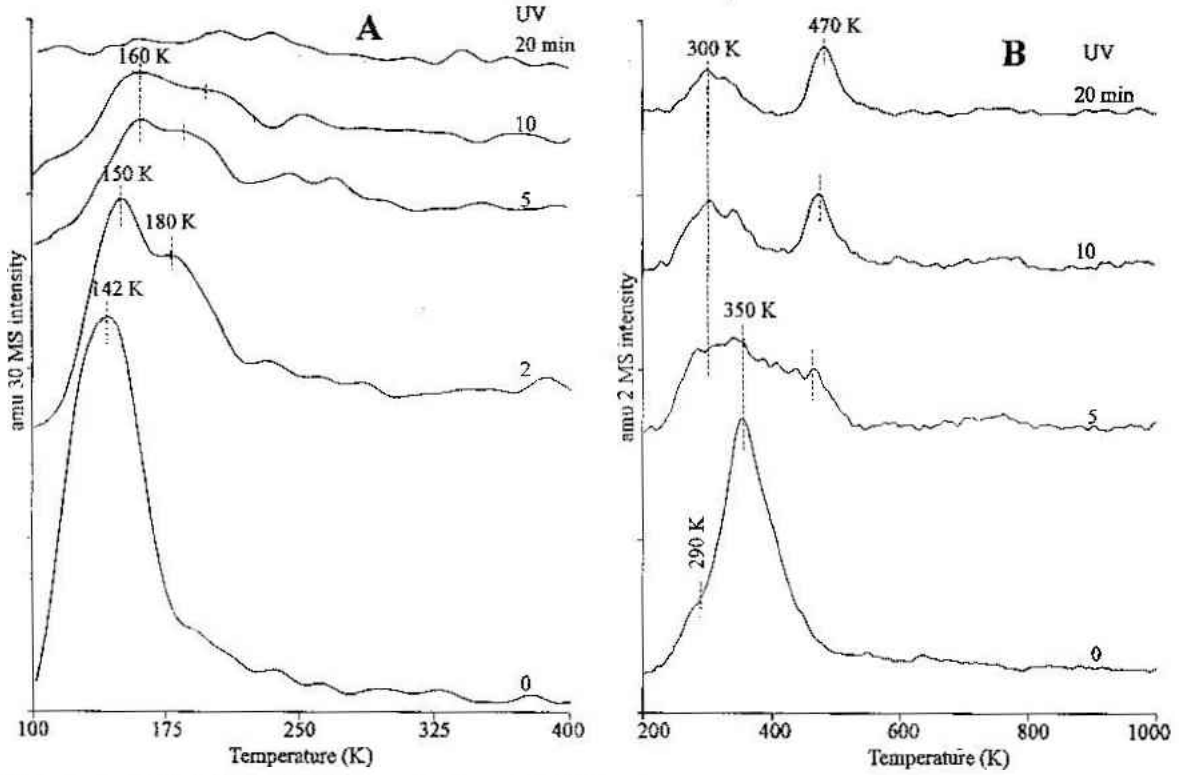

Figure 5. TPD spectra of (A) C_2H_6 and (B) H_2 as a function of irradiation time. The exposure of C_2H_5I was 3.6 L.

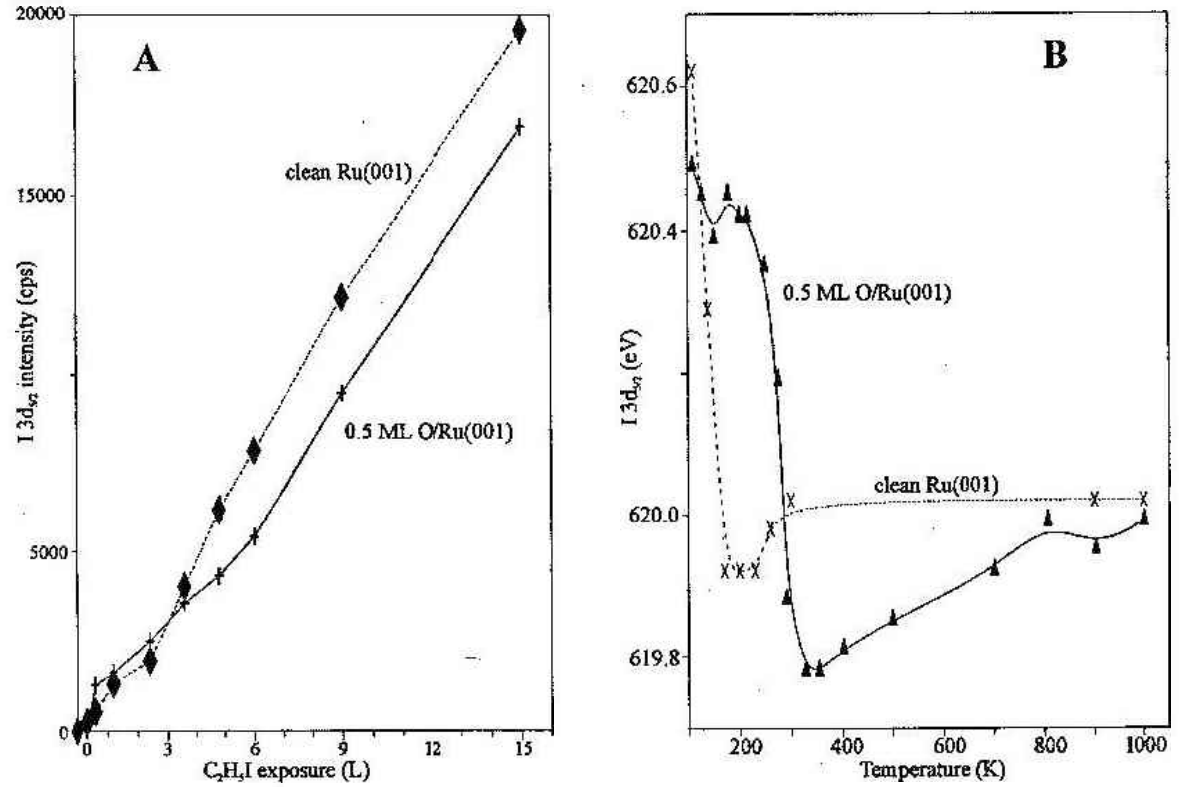

Figure 6. Area of the I($3d_{5/2}$) XP signal as a function of exposure (A) and position of the I($3d_{5/2}$) peak as a function of annealing (B).

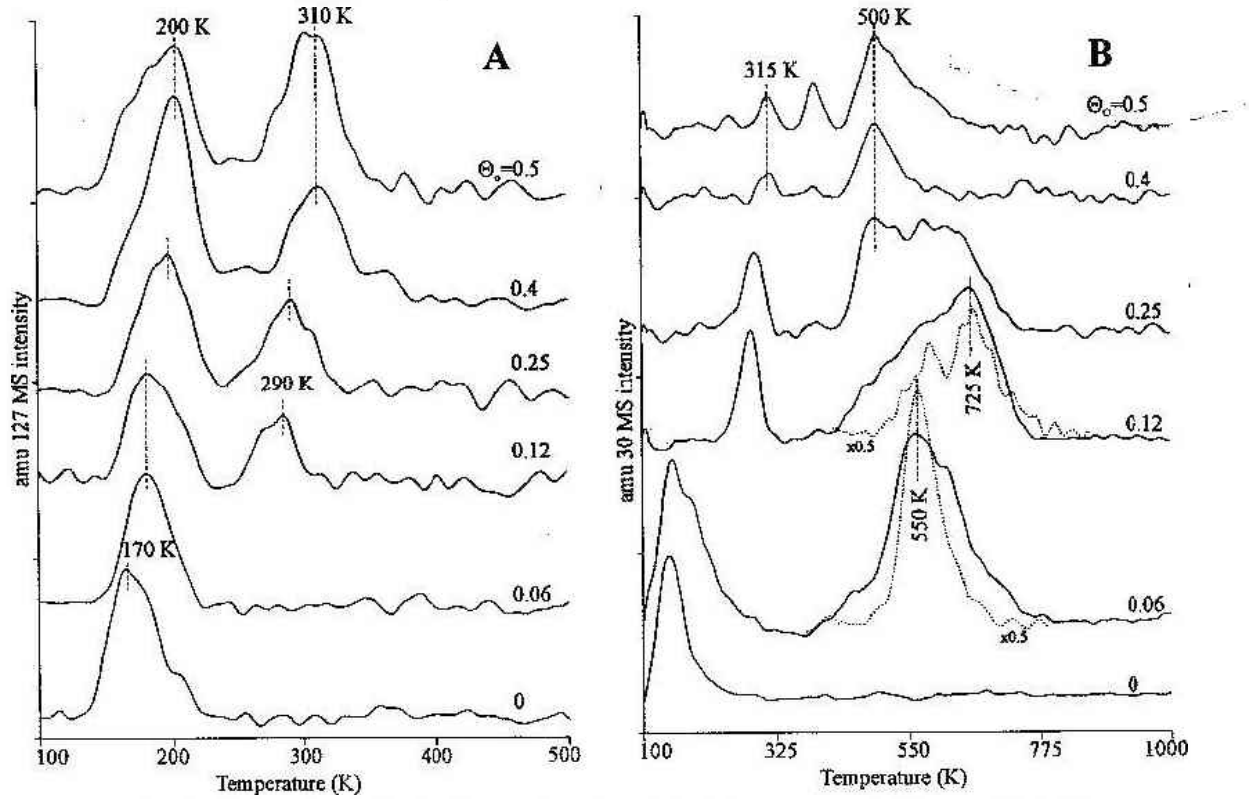

Figure 7. TPD spectra of (A) C_2H_5I and (B) $C_2H_6 + C^{18}O$ as a function of Θ_O. The exposure of C_2H_5I was 3.6 L. The dashed curves in (B) represent the TPD of $C^{18}O$ after annealing the C_2H_5I layer to 400 K (bottom) and 680 K (top), respectively, and post-dosing the sample with O_2. The temperature of O_2 dosing was 110 K.

CHO starts just above 300 K, the main peak is detected at T_P = 405 K. Below Θ_O = 0.25 ML CH_3CHO formation is not observed, but a feature of the 33 amu trace appears (Figure 9B). Its peak temperature coincides with the low-temperature shoulder observed in the 31 amu spectra. Following the 33 amu trace at Θ_O = 0.4−0.5 ML featureless spectra are detected. The characteristics of the spectra mentioned above clearly indicate that two different species are formed during annealing. On the basis of the analysis of mass spectrometric data the 33 amu trace is attributed to diethyl ether ($C_2H_5-{}^{18}O-C_2H_5$), which is produced between Θ_O = 0.12−0.25 ML.

Note that neither CO_2 nor H_2O was detected among the desorption products.

4. Discussion

4.1. Reactions on Clean Ru(001). On the basis of previous measurements on the adsorption of CH_2I_2 on Ru(001)[7] we

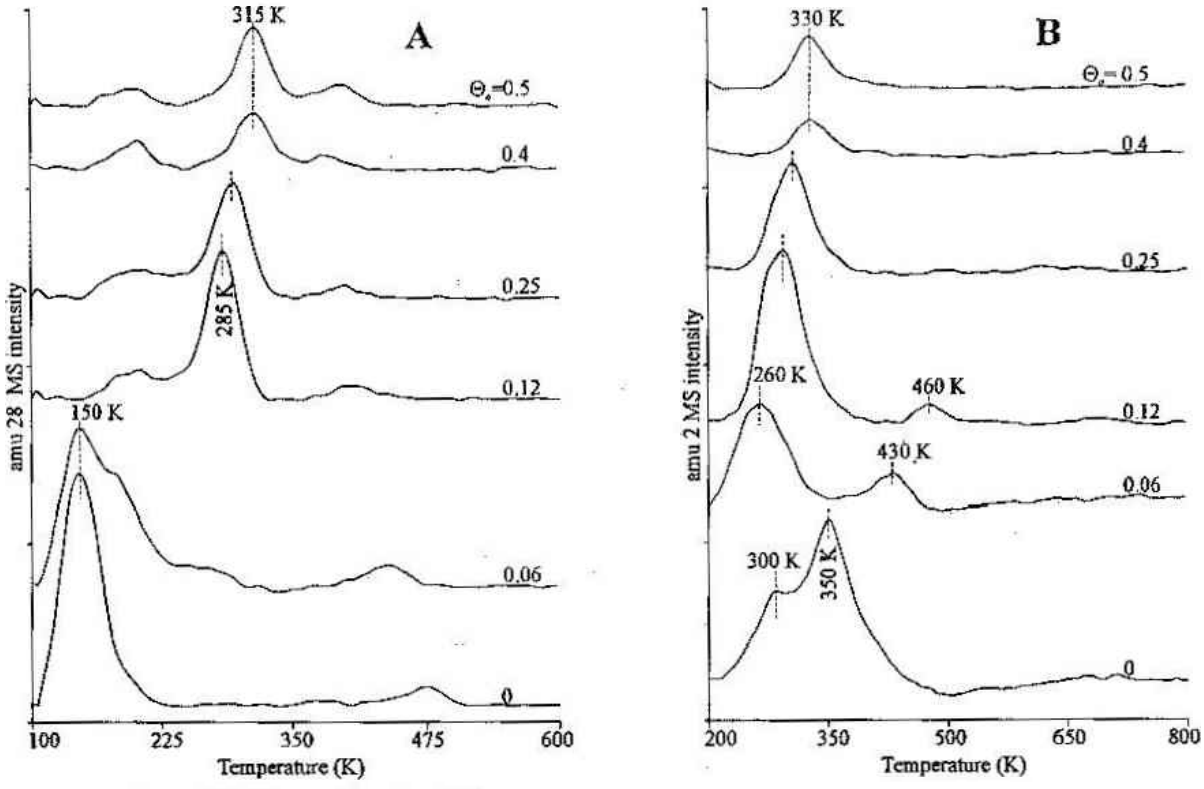

Figure 8. TPD of (A) C_2H_4 and (B) H_2 as a function of Θ_O.

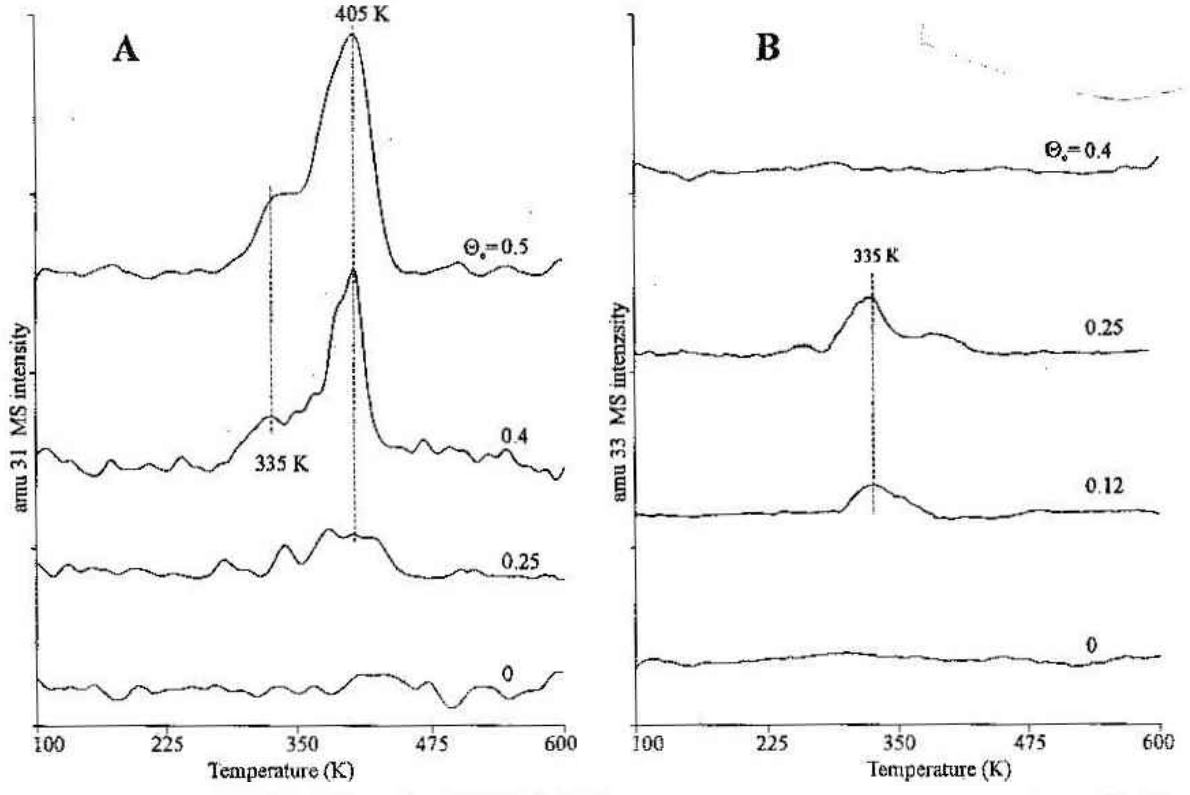

Figure 9. TPD spectra of (A) acetaldehyde (33 amu) and (B) diethyl ether (31 amu) as a function of Θ_O. The exposure of C_2H_5I was 3.6 L.

assumed that C_2H_5I molecules also bond to the surface via their iodine side. This proposal is supported by the studies of C_2H_5I adsorption on several transition metal surfaces.[13,14,22]

The binding energy of I($3d_{5/2}$) at 621.0 eV obtained at and above 2.4 L of C_2H_5I exposure at 110 K (Figure 1A), corresponds to iodine in the molecularly bonded C_2H_5I.[5,6,23,24] At lower exposures the peak appeared at 620.4 eV, which may indicate the dissociation of C−I bond. The shift of the I($3d_{5/2}$) peak occurs to lower binding energies at 150 K (Figure 1B), suggesting the cleavage of the C−I bond and consequently the formation of atomic I on the surface.[5,6,23,24]

The desorption features of the parent show an interesting phenomenon with increasing dose (Figure 2A). The peak labeled β_2 appears first and its T_P is higher by approximately 20 K than that of β_1. The relative intensity of the two peaks is approximately 1. We may assume that the existence of β_1 and β_2 originates from the intermolecular interactions in the adsorbed layer, forming a two-dimensional islandlike structure. The β_2 peak may be assigned to C_2H_5I molecules bonded independently or adsorbed in the perimeter of the islands, while the peak labeled with β_1 corresponds to molecules desorbing from the inside of the islands. However, the highly polar molecules, such

as alkyl halides, adsorbed next to each other are not expected to form islands spontaneously due to the strong dipole−dipole repulsion among neighbors. Therefore, it is a more plausible explanation that the separate desorption peaks of C_2H_5I (β_2, and β_1) can be attributed to the formation of a bilayer. Above 3 L exposure a second layer (β_1) starts to develop on top of the first chemisorbed phase (β_2), probably with opposite orientation (ethyl down). Similar structure were concluded for CH_3Br[25] and CH_3Cl[26] on Ru(001) and for C_2H_5Cl[27] on Pt(111). The α peak corresponds to the condensed multilayer, which starts to build up on the top of the bilayer.

As the C−I bond breaks, the liberated C_2H_5 groups immediately transform further. There are two competitive reaction pathways for them: (i) dehydrogenation to ethylene, very likely to di-σ-C_2H_4, and (ii) hydrogenation to C_2H_6. This latter species is observed in TPD spectra following the 30 amu trace (Figure 2B). It implies that the dehydrogenation process also occurs as H is necessary for the formation of C_2H_6. This reaction, however, is not stopped at the stage of di-σ-C_2H_4, but another species, ethylidyne (CCH_3) is produced quickly. The formation of the latter compound is supported by the complex structure of the H_2 desorption curves (Figure 3). Similar structure was observed following the adsorption CH_2I_2, CH_3I, and C_2H_4 over Ru(001) and was ordered to the formation and decomposition of CCH_3.[7,8,28,29]

Accordingly, the observed asymmetric peak shifting from 405 to 350 K originates from the associative desorption of H atoms produced in the dehydrogenation of C_2H_5 and di-σ-C_2H_4:

$$C_2H_{5(a)} \rightarrow C_2H_{4(a)} + H_{(a)}$$

$$C_2H_{4(a)} \rightarrow CCH_{3(a)} + H_{(a)}$$

This peak temperature agrees with that measured following H_2 adsorption on the same surface.[30] At larger exposures (above 2.4 L), the concentration of the decomposition products is significantly increased, the surface is assumed to be overcrowded with I(a), H(a), and CCH_3(a) at 300 K. The crowded surface causes the H(a) to desorb from a compressed overlayer at lower temperature with $T_P = 290$ K.[31] At the same time the intensity of the peak at $T_P = 350-340$ K depresses, and new peak, $T_P =$ 400 K, emerges on its high-temperature side.

It has been revealed before that the coadsorbed species significantly modifies the thermal stability of CCH_3.[32−34] We assume the adsorbed I has the same effect, i.e., stabilizes the CCH_3 species (occupying 3-fold hollow sites with the C_3 axis parallel with the surface normal) not allowing to tilt the C−C axis toward the surface. Accordingly, the $T_P = 340-350$ K desorption feature is attributed to the decomposition of CCH_3 not influenced by coadsorbed I(a) and the new peak at 400 K peak exhibits the stabilizing effect of I(a). The decomposition of CCH_3 is assumed to occur in a stepwise manner: the clearly detectable intermediates are CCH(a)[34] and CH(a).[35] The dehydrogenation of this latter species takes place above 500 K resulting in a broad H_2 desorption feature. Above 700 K there is only C(a) and I(a) left on the surface. The C(a) is assumed to be carbidic,[35] which may transform to a graphite-like phase above 900 K.

The integrated intensities of the different H_2 desorption features (after deconvolution of the measured curves to physically reasonable number of peaks) offer a rough estimation on the relative rate of the dehydrogenation−hydrogenation processes of adsorbed C_2H_5. Accepting the previous consideration the integrated area of the peaks with $T_P = 340$ and 400 K relates to the decomposition of CCH_3. On the other hand, the area of the $T_P = 290$ K peak is proportional to the difference of the CCH_3 and C_2H_6 produced as the evolution of C_2H_6 consumes some H supplied by the formation of CCH_3 from C_2H_5 groups. This calculation showed that the relative amount of CCH_3 increases with increasing exposure. At 4.8 L 63% of the decomposed C_2H_5 species is hydrogenated and 37% gives CCH_3. At monolayer coverage (6 L) these values are 57% and 43% which does not change significantly at higher doses.

4.2. Effects of Illumination. UV illumination affects drastically the adsorption and decomposition characteristics of C_2H_5I. As was demonstrated by the XP spectra in Figure 4, it promotes the dissociation of C_2H_5I even at 110 K. Comparing the I($3d_{5/2}$) XP signal intensities after annealing to 700 K with and without irradiation the dissociation of the C−I bond is found to be higher by 60% for the irradiated sample.

The reaction pathways of the C_2H_5 groups produced at 110 K are also modified as a result of irradiation as indicated by the C_2H_6 and H_2 desorption spectra (Figure 5). The hydrogenation process continuously decreased and no C_2H_6 was detected after 10 min illumination. The desorption of H_2 is also altered. After 5 min irradiation a broad feature emerged comprised of at least three different states. Longer illumination causes vanishing of the original $T_P = 350$ K peak, while the features at $T_P = 300$ K and $T_P = 470$ K become clearly distinguishable. As was revealed by XPS results, following the UV illumination I(a) is produced in high concentration even at 110 K, which leads to the more pronounced stabilization of CCH_3. This is indicated by the higher T_P (470 K) of H_2. At the same time the amount of C_2H_6 desorbed from the surface is totally suppressed. This suggest that the high local coverage of I(a) favors the dehydrogenation reaction producing CCH_3, which was also observed in dark experiments at higher initial doses.

4.3. Reaction Pathways on O/Ru(001). The sticking coefficient of C_2H_5I is independent of the O coverage for low exposures (Figure 6A). Above 3.6 L dose a larger number of molecules is to be attached to the surface, but the predosed O reduces the number of available sites by occupying a part of the 3-fold hollow sites, thus explaining the difference between the curves in Figure 6A. The adsorbed O atoms possess a partial negative charge which interact with the opposite by charged particles such as the carbon center of C_2H_5I species. This short-range Coulomb interaction accounts for the shift of the C−I bond breaking and parent desorption to higher temperature (Figures 6B and 7A). From the data of the XP spectra (Figure 6B) we find that the rupture of the C−I bond in the coadsorbed layer is completed by 325 K.

The preadsorbed O(a) exerts not only a stabilization influence, but it also opens channels for the formation of several new products. The relative intensities of the 28 and 30 masses unambiguously indicate the release of C_2H_4, which was not observed on the clean surface (Figure 8A). The amount of hydrocarbons desorbed from the surface reaches its maximum at $\Theta_O = 0.12-0.25$ ML. There are O-patches characterized by diffuse p(2 × 2) LEED pattern at this O coverage and $\Theta_O =$ 0.25 ML is necessary for the appearance of the sharp p(2 × 2) image.[21,36] (The surface saturated with O under UHV conditions has a p(1 × 2) LEED structure with $\Theta_O = 0.5$ ML.)

We suspect that the presence of O patches is responsible for the coincident formation of C_2H_6, C_2H_4, and H_2. The side-chains of the C_2H_5I molecules bonded next to the O islands get further from the surface, consequently the C−H bonds become less activated. The average lifetime of the C_2H_5 groups produced by C−I bond breaking of the stabilized molecules is increased and the dehydrogenation processes slow. The cleavage of the

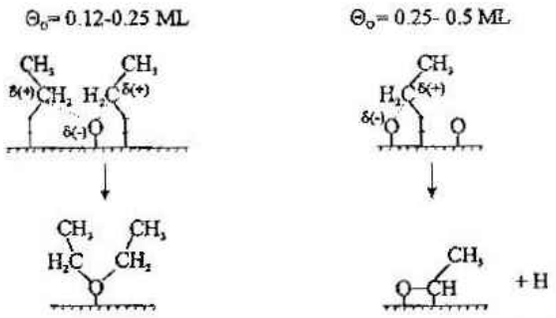

Figure 10. Schematic diagram for the formation of diethyl ether and acetaldehyde on O-covered Ru(001).

C−I bond takes place above 250 K when the C_2H_4 molecules desorb from the Ru(001) surface.[35,37,38] The C−I bond breaks presumably in S_{N2} reaction between O(a) and C_2H_5I(a) as the different desorption products appear in a narrow temperature regime indicating that the bond cleavage and the desorption occur instantly. The H liberated in the dehydrogenation reaction can couple with an intact C_2H_5 group to give C_2H_6 or with another H resulting in H_2, respectively. This latter possible reaction is indicated by the desorption of H_2 between 260 and 350 K as shown by the spectra in Figure 8B. The desorption temperature of H_2 is lower than expected from a crowded surface, but the coadsorbed O is known to have a similar effect.[39]

The appearance of C_2H_4 among the desorption products suggests that the H-affinity of the ruthenium surface is reduced on O-covered surface. The reduced H-affinity of the O-modified surface is also indicated by the fact that the H_2 desorption features characteristic of the decomposition of geometrically stabilized CCH_3 (T_P > 400 K) loose their intensities with respect to the low-temperature H_2 desorption peak (T_P = 260−300 K). This observation shows that the amount of C_2H_4 increases at the expense of CCH_3. Oxygen atoms also prevent the CCH_3 species from tilting toward the surface which shifts its decomposition temperature to higher values. The appearance of the T_P = 430 and 460 K peaks relates to the increased stability of CCH_3. At the same time that the area of this H_2 desorption peak continuously decreases with increasing O coverage. Moreover, there is no detectable feature indicating the presence of CCH_3 on the surface above Θ_O = 0.12 ML. This behavior agrees with our assumption that the formation of CCH_3 is suppressed above this O coverage and the reduced amount of CCH_3 species decomposes along a new reaction route (see below). The H_2 desorption spectra detected above Θ_O = 0.12 ML suggest the concomitant formation of H_2, C_2H_6, and C_2H_4 as discussed above.

An interesting feature of the C_2H_5 + O/Ru(001) system is the appearance of oxygenated hydrocarbons, acetaldehyde, and diethyl ether, in the products of the surface reaction (Figure 9). At lower O concentration diethyl ether (33 amu) is produced in the interaction of atomic oxygen with two ethyl groups. At higher O coverage the formation of acetaldehyde comes into prominence. This process provides less amount of H_2 than the decomposition of CCH_3. The reaction schemes for the formation of diethyl ether and acetaldehyde are represented in Figure 10.

In addition to above-mentioned compounds we also detected the formation of CO at high temperature (T_P = 500−725 K). To find out the source of its formation we executed some control measurements. Ru(001) surface was presaturated with C_2H_5I, annealed to 400 K to give CCH(a),[34,38] and dosed with $^{18}O_2$ at 110 K. The desorption of $C^{18}O$ produced (indicated by dashed lines in Figure 7B) coincides with the spectrum of CO registered before at Θ_O = 0.06 ML. This coincidence suggests that the oxidation of CCH(a) to CO is responsible for this peak. In the next experiment, adsorbed C_2H_5I was annealed to 680 K to form CH(a) species,[35] and dosed with $^{18}O_2$ at 110 K. In this case the TPD spectrum of CO resembled that one obtained at Θ_O = 0.12 (Figure 7B).

This behavior reveals that adsorbed O caused also the rupture of the C−C bond in CCH at Θ_O =0.12−0.25 before its oxidation. Note that at this coverage the well-ordered p(2 × 2)-O structure of adsorbed O is formed.[21,36] At higher oxygen coverage, Θ_O =0.4−0.5, the dominant process is the selective oxidation of C_2H_5 to acetaldehyde, and the formation and reaction of CCH_3 are largely suppressed. In harmony with this, the above CO peaks are missing.

UV illumination of the coadsorbed layer does not affect the subsequent TPD product distribution which reflects that the UV photons are incapable of destroying the structure of the O and C_2H_5I species held together by Coulomb interatomic forces.

4.4. Comparison of Surface Chemistry of Methylene, Methyl, and Ethyl Groups on Ru(001). On the basis of the data obtained we may compare the behavior of the C_2H_5 group with that of CH_3[8] and CH_2[7] moieties on the same surface. It is common for all three species that they are easily formed from the dissociation of their corresponding iodo compounds even at low temperatures and undergo hydrogenation and dehydrogenation reactions at higher temperatures. In contrast to the other platinum metals, C−C bonds are formed during thermally activated surface rearrangement of adsorbed CH_2 and CH_3. Such kind of coupling reaction was not observed for the ethyl species. In all three cases, ethylidyne, (CCH_3(a)) is produced in the dehydrogenation process especially at higher coverage. Its stability is independent of the parent hydrocarbon fragments but it is influenced by coadsorbed iodine.

Preadsorbed oxygen significantly modified the reaction pathway of alkyl groups. The formation of ethylidyne is suppressed by the oxygen atoms. The products of partial oxidation is influenced by the number of carbon atoms. The methylene groups (very probably CH_3 also) react with coadsorbed oxygen forming formaldehyde, the ethyl species gives diethyl ether and acetaldehyde depending on the structure and concentration of surface oxygen.

5. Conclusion

TPD and XPS measurements revealed that the uptake of C_2H_5I is affected only slightly by the O coverage of the Ru(001) surface. Thermal cleavage of the C−I bond begins at 130 K, yielding adsorbed I and C_2H_5. The latter is transformed into CCH_3(a) and C_2H_6(g) depending on the surface coverage. UV illumination enhances the low-temperature dissociation and causes a significant stabilization on the adsorbed CCH_3 groups through the homogeneously dispersed iodine atoms formed. Preadsorbed O also stabilizes the C_2H_5I species, and delays their desorption and dissociation as well. It decreases the affinity of H to the surface and facilities the breaking of C−C bond. It reacted with C_2H_5 to give acetaldehyde and diethyl ether.

Acknowledgment. This work was supported by OTKA Grant T32040.

References and Notes

(1) Bibby, D. M.; Chang, C. D.; Howe, R. F.; Yurchak S. (Eds.) In *Studies in Surface Science and Catalysis*; Delmon, B., Yates, J. T., Jr., Eds; Elsevier: Amsterdam, 1988; Vol. 36
(2) Steinbach, F.; Kiss, J.; Krall, R. *Surf. Sci.* **1985**, *157*, 401.
(3) Zhou, X.-L.; Zhu, X.-Y.; White, J. M. *Surf. Sci. Rep.* **1991**, *13*, 73.
(4) Zaera, F. *Acc. Chem. Res.* **1992**, *25*, 260.

(5) Bent, B. E. *Chem. Rev.* **1996**, *96*, 1361.
(6) Solymosi, F. *J. Mol. Catal.* **1998**, *131*, 121.
(7) Kis, A.; Smith, K. C.; Kiss, J.; Solymosi, F. *Surf. Sci.* **2000**, *460*, 190.
(8) Zhou, Y.; Henderson, M. A.; Feng, W. M.; White, J. M. *Surf. Sci.* **1989**, *224*, 386.
(9) Kis, A.; Kiss, J.; Solymosi, F. *Surf. Sci.* **2000**, *459*, 149.
(10) Zaera, F.; Hoffmann, H.; Griffiths, P. R. *Vacuum* **1990**, *41*, 735.
(11) Zaera, F. *J. Phys. Chem.* **1990**, *94*, 8350.
(12) Hoffmann, H.; Griffiths, P. R.; Zaera, F. *Surf. Sci.* **1992**, *262*, 141.
(13) Solymosi, F.; Bugyi, L.; Oszkó, A. *Langmuir* **1996**, *12*, 4145.
(14) Kovács, I.; Solymosi, F. *J. Phys. Chem.* **1993**, *97*, 11056.
(15) Solymosi, F.; Bugyi, L.; Oszkó, A.; Horváth, I. *J. Catal.* **1999**, *185*, 160.
(16) Zhou, X.-L.; White, J. M. *Catal. Lett.* **1989**, *2*, 375.
(17) Liang, J. J.; Bent, B. E. *J. Am. Chem. Soc.* **1993**, *115*, 6943.
(18) Yang, M. X.; Jo, S. K.; Paul, A.; Avila, L.; Bent, B. E.; Nishikida, K. *Surf. Sci.* **1995**, *325*, 102.
(19) Bol, C. W. J.; Friend, C. M. *J. Phys. Chem.* **1995**, *99*, 11930.
(20) Bugyi, L.; Oszkó, A.; Solymosi, F. *J. Catal.* **1996**, *159*, 305.
(21) Winterlin, J.; Trost, J.; Renisch, S.; Schuster, R.; Zambelli, T.; Ertl, G. *Surf. Sci.* **1996**, *394*, 159.
(22) Jenks, C. J.; Bent, B. E.; Bernstein, N.; Zaera, F. *J. Phys. Chem. B* **2000**, *104*, 3008.
(23) Solymosi, F.; Révész, K. *J. Am. Chem. Soc.* **1991**, *113*, 9145.
(24) Buelow, M. T.; Immaraporn, B.; Gellman, A. J. *J. Catal.* **2001**, *203*, 41.
(25) Livneh, T.; Asscher, M. *J. Phys. Chem.* B **1997**, *101*, 7505.
(26) Livneh, T.; Lilach, Y.; Asscher, M. *J. Chem. Phys.* **1999**, *111* (24), 11138.
(27) Sam, K. Jo.; Kiss, J.; Polanco, J. A.; White, J. M. *Surf. Sci.* **1991**, *253*, 233.
(28) Barteau, M. A.; Broughton, J. Q.; Menzel, D. *Appl. Surf. Sci.* **1984**, *19*, 92.
(29) Greenlief, C. M.; Radloff, P. L.; Zhou, X.-L.; White J. M. *Surf. Sci.* **1987**, *191*, 93.
(30) Shimizu, H.; Christmann K.; Ertl, G. *J. Catal.* **1980**, *61*, 412.
(31) Peebles, D. E.; Schreifels, J. A.; White, J. M. *Surf. Sci.* **1982**, *116*, 117.
(32) Mimn, C. A.; Weisel, M. D.; Hoffmann, F. M.; Sinfelt, J. H.; White, J. M. *J. Phys. Chem.* **1993**, *97*, 12656.
(33) Hills, M. M.; Parmeter, J. E.; Weinberg, W. H. *J. Am. Chem. Soc.* **1986**, *108*, 7215.
(34) Henderson, M. A.; Mitchell, G. E.; White, J. M. *Surf. Sci.* **1988**, *203*, 378.
(35) Livneh, T.; Asscher, M. *J. Phys. Chem. B* **2000**, *104*, 3355.
(36) Madey, T. E.; Engelhardt, E.; Menzel, D. *Surf. Sci.* **1975**, *48*, 304.
(37) Rahman, T. S.; Anton, A. B.; Avery, N. R.; Weinberg, W. H. *Phys. Rev. Lett.* **1983**, *51*.
(38) Hills, M. M.; Parmeter, J. E.; Mullins, C. B.; Weinberg, W. H. *J. Am. Chem. Soc.* **1986**, *108*, 3554.
(39) Hrbek, J. *J. Catal.* **1986**, *100*, 523.